Nature of the Asymmetry in the Hydrogen-Bond Networks of Hexagonal Ice and Liquid Water

ARTICLE *in* JOURNAL OF THE AMERICAN CHEMICAL SOCIETY · FEBRUARY 2014

Impact Factor: 12.11 · DOI: 10.1021/ja411161a · Source: PubMed

2 AUTHORS:

Thomas D Kühne
Universität Paderborn
64 PUBLICATIONS **1,135** CITATIONS
SEE PROFILE

Rustam Khaliullin
McGill University
29 PUBLICATIONS **2,465** CITATIONS
SEE PROFILE

JACS
JOURNAL OF THE AMERICAN CHEMICAL SOCIETY
Article
pubs.acs.org/JACS

Nature of the Asymmetry in the Hydrogen-Bond Networks of Hexagonal Ice and Liquid Water

Thomas D. Kühne and Rustam Z. Khaliullin*

Institute of Physical Chemistry and Center for Computational Sciences, Johannes Gutenberg University of Mainz, Staudinger Weg 7, 55128 Mainz, Germany

Supporting Information

ABSTRACT: The interpretation of the X-ray spectra of water as evidence for its asymmetric structure has challenged the traditional nearly tetrahedral model and initiated an intense debate about the order and symmetry of the hydrogen-bond network in water. Here, we present new insights into the nature of local interactions in ice and liquid water obtained using a first-principle energy decomposition method. A comparative analysis shows that the majority of molecules in liquid water in our simulation exhibit hydrogen-bonding energy patterns similar to those in ice and retain the four-fold coordination with only moderately distorted tetrahedral configurations. Although this result indicates that the traditional description of liquid water is fundamentally correct, our study also demonstrates that for a significant fraction of molecules the hydrogen-bonding environments are highly asymmetric with extremely weak and distorted bonds.

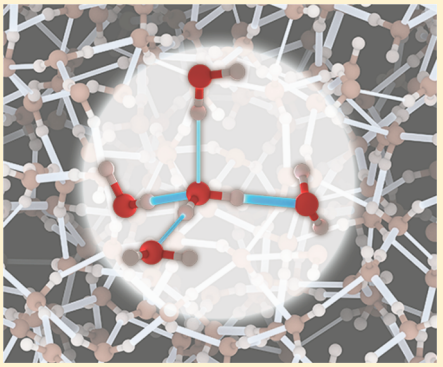

INTRODUCTION

Liquid water is of paramount importance for life on Earth. Therefore, its properties and behavior have been a subject of extensive scientific investigation. Numerous studies of the local structure of liquid water at ambient conditions, based on a wide range of experimental and computational techniques,[1] have long supported a view that water molecules are bonded, on average, to four nearest neighbors in distorted tetrahedral configurations.[2,3] This traditional picture has recently been questioned based on a comparative analysis of the X-ray absorption spectra of water and ice.[4] The study suggested that, in the liquid phase, most molecules experience highly asymmetric environments and form strong hydrogen bonds (HBs) with only two neighbors.[4,5] However, the asymmetric model of water, often referred to as the "chains and rings" model, has been challenged on many fronts,[3] and the order and symmetry of the HB network in water remain subjects of an intense scientific debate.[3,5]

Recently, we have employed the energy decomposition analysis based on absolutely localized molecular orbitals (ALMO EDA)[6] to study the HB network in liquid water at ambient conditions.[7] The unique ability of ALMO EDA to characterize the strength of individual HBs has been used to show that although a water molecule forms, on average, two strong donor and two strong acceptor bonds, thermal distortions induce a significant instantaneous asymmetry in the strength of these contacts. According to ALMO EDA, the strongest donor (acceptor) contact of a molecule is approximately twice as strong as the other donor (acceptor) bond. Here, we present results of a comparative ALMO EDA study of water and hexagonal ice that reveals the full complexity of the origins of the observed asymmetry and provides a deeper insight into the structure of the HB network in liquid water.

COMPUTATIONAL METHODS

ALMO EDA separates the total interaction energy of molecules (ΔE_{TOT}) into the interaction energy of the unrelaxed electron densities on the molecules (ΔE_{FRZ}) and the density relaxation energy. The latter can be further decomposed into an intramolecular polarization associated with deformation of the electron clouds on molecules in the field of each other (ΔE_{POL}), two-body donor–acceptor interactions (ΔE_{DEL}), and a negligibly small higher-order (ΔE_{HO}) relaxation term (see ref 6 for a detailed description of the ALMO EDA terms).

$$\Delta E_{TOT} = \Delta E_{FRZ} + \Delta E_{POL} + \Delta E_{DEL} + \Delta E_{HO}$$

$$\Delta E_{DEL} = \sum_{C=1}^{Mol} \Delta E_C = \sum_{A,D=1}^{Mol} \Delta E_{D\to A}$$

The two-body components $\Delta E_{D\to A}$ are the main focus of this work. They arise due to delocalization of electrons from the occupied orbitals of donor molecule D to the virtual orbitals of acceptor A. Being highly sensitive to distortions of the HBs, each two-body term is an excellent descriptor of the strength of an individual HB in the network. The electron delocalization energy per molecule ΔE_C can be analyzed by considering each water molecule as a donor or as an acceptor:

$$\Delta E_C = \sum_{N=1}^{Mol} \Delta E_{C\to N} = \sum_{N=1}^{Mol} \Delta E_{N\to C}$$

Received: August 15, 2013
Revised: November 1, 2013
Published: February 12, 2014

where C is the central molecule and N is its neighbors. In this paper, terms donor and acceptor are used to describe the role of a molecule in the transfer of the electron density. This is opposite to the labeling used for a donor and an acceptor of hydrogen in a HB.

Configurations for ALMO EDA were obtained from ring-polymer molecular dynamics simulations[8] based on the ab initio-derived TPSS-D3-FF potential.[9] The simulations were designed to reproduce the dispersion interactions between the water molecules as well as the nuclear quantum effects, both of which improve the description of the local structure of water.[10] The simulations were performed at constant temperature and density: 268 K and 0.918 g/cm^3 for hexagonal ice and 298 K and 0.997 g/cm^3 for liquid water.[11] ALMO EDA was carried out using the BLYP functional[12] for 5001 snapshots for each phase. A detailed description of the calculations is presented in the Supporting Information.

RESULTS AND DISCUSSION

Figure 1 shows the average delocalization energy per molecule $\langle \Delta E_C \rangle$ (the total height of the columns) together with its

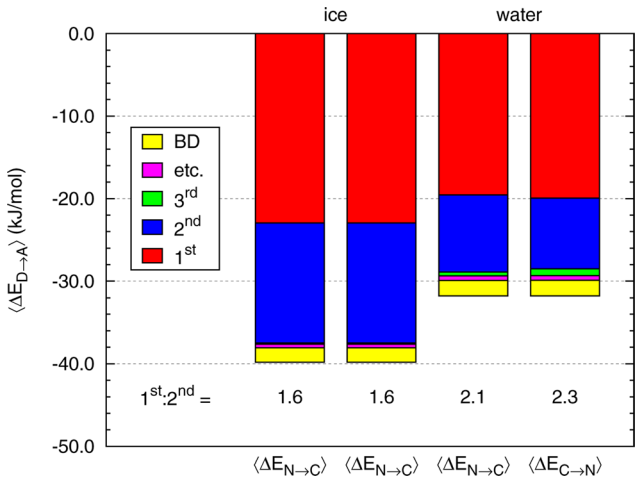

Figure 1. Average contributions of the three strongest acceptor $\langle \Delta E_{N\to C} \rangle$ and donor $\langle \Delta E_{C\to N} \rangle$ interactions to the total delocalization energy $\langle \Delta E_C \rangle$. The fourth, fifth, and other terms are denoted with "etc.". "BD" refers to the combined back-donation terms.

decomposition into individual interactions arranged in the order of decreasing strength. In both ice and water, the electron delocalization is dominated by two strong intermolecular contacts, which together are responsible for 95% (ice) and ~90% (liquid) of the delocalization energy of a single molecule. In ice, the third strongest donor (acceptor) interaction contributes only 0.4% to $\langle \Delta E_C \rangle$, whereas, in the liquid phase, its contribution is increased to 1.4−2.6%, which indicates the presence of overcoordinated molecules. The remaining term ("etc." in Figure 1) comes from interactions with the second and more distant coordination shells and contains numerous individually small contributions that together account for 1.0% in ice and 1.8% in the liquid. The relatively large "BD" term in Figure 1 arises from back-donation of electrons from typical acceptors to typical donors[13] (see the Supporting Information).

As evident from Figure 1, a high degree of disorder in the HB network in the liquid phase results in a substantial decrease of the average strength of the donor−acceptor interactions. Despite this difference, there is a striking similarity in the relative energies of individual contacts. In both liquid and solid phases, a typical water molecule experiences a significant asymmetry in the strength of its two main donor−acceptor interactions: their ratio is 1.6 in ice and 2.2 in water (Figure 1).

To understand the origins of the high asymmetry in ice, which is generally regarded as a solid with symmetric HBs, we analyzed the joint distribution of molecules according to the strength of the first two strongest interactions (Figure 2). We

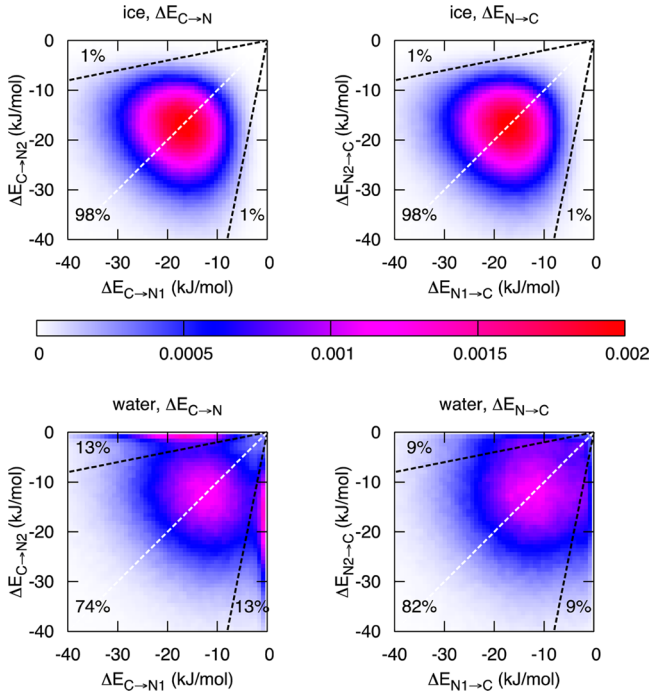

Figure 2. Distribution of molecules in ice and liquid water according to the strength of the first two strongest donor ($\Delta E_{C\to N}$) and acceptor ($\Delta E_{N\to C}$) interactions. X or Y axis is assigned randomly, i.e., independently from the HB energies. The dashed white lines are the lines of the ideal symmetry $\gamma_D = 0$ and $\gamma_A = 0$. The dashed black lines correspond to $\gamma_D = 0.8$ and $\gamma_A = 0.8$.

used dimensionless asymmetry parameters γ_D and γ_A to simplify the discussion;[7] γ_D characterizes the asymmetry of the two strongest donor contacts of a molecule:

$$\gamma_D = 1 - \Delta E_{C\to N^{2nd}} / \Delta E_{C\to N^{1st}}$$

where γ_D is 0 if the two contacts are equally strong and equals 1 if the second donor contact does not exist. The γ_A is an equivalent parameter for the acceptor interactions; $\gamma_D = \gamma_A = 0.8$, which is often used below, indicates that the strongest donor or acceptor contact is 5 times stronger than the second strongest contact.

The joint distribution of the strength of the two HBs (Figure 2) in ice is characterized by the peak centered at 18.7 kJ/mol, large deviation from the average values (σ = 7.2 kJ/mol), and a correlation coefficient of 0.1. Such a small correlation coefficient indicates that the two HBs are essentially independent from each other and the asymmetry in ice arises trivially from the very broad distribution of HBs' strengths. As in the case of liquid water,[7] this asymmetry is a result of thermal fluctuations around the average symmetric structure. A detailed time relaxation analysis shows that these fluctuations have a characteristic relaxation time scale of several hundreds of femtoseconds (see ref 7 and the Supporting Information for details).

The distribution of the strength of the donor interactions in the model of liquid water exhibits a drastically different pattern with two pronounced features. In addition to a broad peak

dx.doi.org/10.1021/ja411161a | J. Am. Chem. Soc. 2014, 136, 3395−3399

resembling the one for ice, there is a sharp peak in the region of high γ_D. The center of the first peak is shifted to lower energies (~12 kJ/mol) and is somewhat broader than that of ice. The second peak indicates the presence of molecules with one intact and one broken donor HB ($\Delta E_{C\rightarrow N}$ < 1 kJ/mol). To estimate a fraction of molecules responsible for the sharp asymmetric feature, we draw a somewhat arbitrary boundary at γ_D = 0.8 (dashed line in Figure 2), which divides the distribution into the regions of ice-like configurations and highly asymmetric configurations. Figure 2 shows that 26% of molecules in the liquid phase are characterized with γ_D > 0.8 compared to 2% in ice.

The fraction of molecules with broken acceptor bonds is also significant (18% with γ_D > 0.8), but the distribution of the acceptor interactions does not exhibit a high-γ_A peak, which would match the high-γ_D peak. This difference indicates that in broken HBs only the donor of electrons remains undercoordinated while the acceptor (i.e., hydrogen atom) forms a HB with another donor that becomes overcoordinated. The existence of a significant fraction of overcoordinated donors is supported by a relatively large contribution of the third interaction shown in Figure 1. It is important to note that the difference between the donor and acceptor interactions seen in Figures 1 and 2 is consistent with the well-known fact that the distribution of electron acceptors around a water molecule is more disordered than that of the donors.[14] This phenomenon is attributed to the existence of the so-called "negativity track" between the lone pairs of a water molecule, which facilitates the disordered motion of electron acceptors around the central donor.[15]

To quantify the degree of geometric distortions associated with the observed electronic asymmetry, we calculated the spatial distribution functions (SDFs) of oxygen atoms. To investigate the asymmetry in the distribution of electron-donating neighbors, we used $\Delta E_{N\rightarrow C}$ to orient the central molecules so that the *x*-coordinates of their strongest donors are always positive (cf. random orientation in regular SDFs[16]). A cross section of the resulting SDFs is shown in the top row in Figure 3. Alternatively, the central molecules can be oriented so that the *y*-coordinates of their strongest acceptors are always positive, emphasizing the asymmetry in the distribution of electron-accepting neighbors (bottom row in Figure 3).

The SDFs obtained by averaging over all central molecules in our model of liquid water are labeled "ALL" in Figure 3. On the geometric scale, the average instantaneous asymmetry is not as pronounced as on the energy scale: the distributions of the strongest and the second strongest donors and acceptors are quite similar. The average intermolecular oxygen−oxygen distances for the strongest (solid circles) and second strongest (dashed circles) interactions differ only by ~0.2 Å and are close to that in ice (~0.1 Å). Thus, the average distortions of the HBs are not large enough to justify the recently proposed asymmetric model.

We also calculated the SDFs for highly asymmetric molecular configurations characterized by γ_D > 0.8 and γ_A > 0.8 (graphs in Figure 3 with the corresponding labels), which according to our analysis exist in liquid water but not in ice. For these configurations, the geometric asymmetry is significant: the difference in the intermolecular oxygen−oxygen distances for the two strongest interaction is ~0.5 Å, and the range of angular distortions of the second strongest HB is remarkably wide, especially for electron-accepting neighbors.

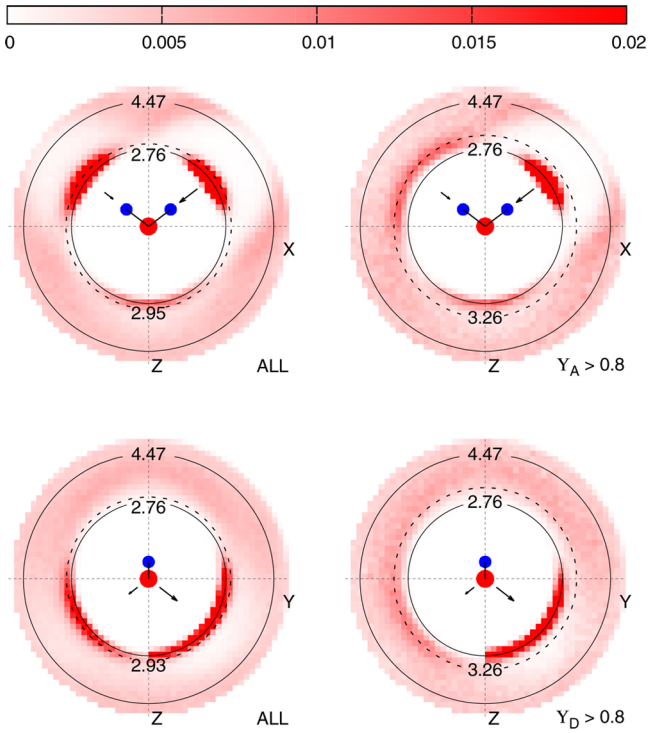

Figure 3. Cross sections of the oxygen SDFs for liquid water. Top row: *x*-direction is chosen toward the strongest donor of electrons to emphasize the asymmetry in the distribution of electron donors. Bottom row: *y*-direction is chosen toward the strongest acceptor of electrons to emphasize the asymmetry in the distribution of electron acceptors. The arrows show schematically the relative strength of donor−acceptor interactions. The label in the bottom right corner of each plot specifies the selection criterion for the central molecules. The solid and dashed circles mark the average positions of the strongest and second strongest donors or acceptors, respectively.

At this point, it is important to comment on the quality of our simulations and the derived results. A comparison of the calculated oxygen radial distribution function (RDF) with recently refined experimental RDFs[17] shows that our simulations produce an overstructured first coordination shell (Figure 4a and Figure S1a in the Supporting Information). Such an overstructuring is typical for RDFs obtained using potentials based on density functional theory since most modern exchange-correlation functionals overestimate the binding energy between water molecules.[18] Integrating the difference between the calculated and experimentally derived RDFs shows that the number of oxygen atoms in the undistorted first coordination shell is overestimated by ~0.12−0.24 (integral from 0 to 2.95 in Figures 4b and S1b), depending on which of the two experimental data sets from ref 17 is used. Assuming that this error results entirely from underestimating the fraction of molecules with highly distorted donor HBs, the percentage of such molecules in real water should be ~12−24% higher than predicted in our simulation. Since approximately half of these unaccounted distorted HBs are donor bonds, the correction gives 38% as an estimate for the fraction of highly asymmetric donor species (i.e., 6−12% higher than 26% obtained in our simulation). The same correction should be applied to the fraction of highly asymmetric acceptor configurations. We would like to note that such an analysis produces only approximate corrections because there exist alternative mechanisms for brining the

dx.doi.org/10.1021/ja411161a | J. Am. Chem. Soc. 2014, 136, 3395−3399

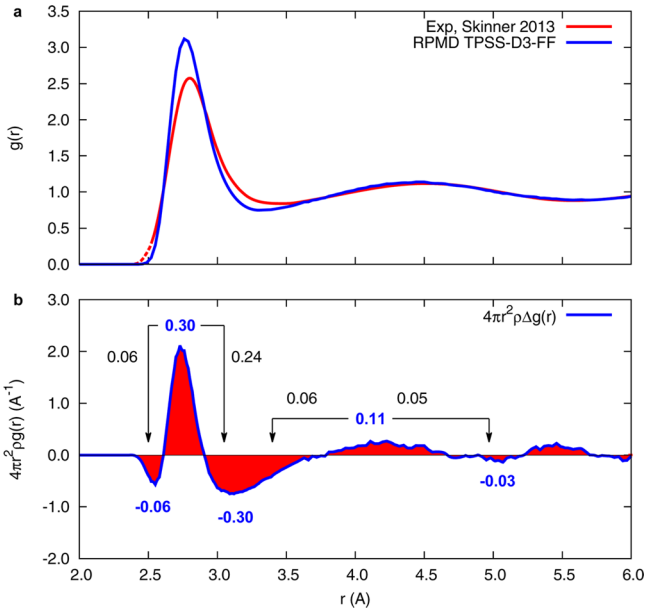

Figure 4. (a) Calculated and experimentally obtained[17b] RDFs of oxygen in liquid water. The dashed red line at ~2.4 Å indicates that additional corrections were made to the experimental RDF (see the Supporting Information). (b) Difference between the RDFs shown in panel a. The numbers in blue show the integrals of the difference for each region of space, whereas black numbers indicate how many oxygen atoms should be redistributed so that the calculated and experimental RDFs match.

simulated RDFs closer to experiment without increasing the fraction of highly asymmetric configurations (see the Supporting Information for details).

It is also important to emphasize that simulations of the same quality as performed in this work are capable of reproducing the X-ray absorption spectra of liquid water with a high degree of accuracy.[19] This is especially important in the present context since it was an interpretation of the X-ray absorption spectra[4] that initiated the ongoing debate around the structure of water. The result of ref 19 implies that despite some shortcomings of the employed theoretical framework our description of the HB network is fundamentally correct. This justifies our conclusion that the fraction of molecules with broken HBs is appreciable but not dominant. Our results are also consistent with the previous studies[4,7,19,20] that demonstrated that only the highly asymmetric configurations are responsible for the distinct pre-edge feature in the X-ray absorption spectra of liquid water, which is mostly absent in ice.

CONCLUSION

In summary, the energy decomposition study presented here shows that, in hexagonal ice, the uncorrelated thermal motion of molecules around their crystallographic sites broadens the range of the HB energies and, thus, creates a noticeable asymmetry in the donor and acceptor contacts of each water molecule. ALMO EDA demonstrates that the majority of molecules in our model of liquid water exhibit HB patterns similar to those in ice and retain the four-fold coordination with only moderately distorted tetrahedral configurations. However, ALMO EDA also reveals the drastic difference between the structure of the HB networks in our models of liquid water and ice. In liquid water, there is a large fraction of molecules with very weak HBs, which are elongated by as much as 0.5 Å and exhibit a wide range of angular distortions.

Our results imply that the traditional view of water as a four-coordinated nearly tetrahedral liquid is more appropriate than the recently proposed asymmetric model. However, the substantial fraction of molecules with broken hydrogen bonds undoubtedly affects physical properties and chemical behavior of liquid water.

ASSOCIATED CONTENT

Supporting Information

Calculated and experimental radial distribution functions, description of molecular dynamics simulations, ALMO EDA calculations, and analysis of the asymmetry relaxation. This material is available free of charge via the Internet at http://pubs.acs.org.

AUTHOR INFORMATION

Corresponding Author

rustam@khaliullin.com

Notes

The authors declare no competing financial interest.

ACKNOWLEDGMENTS

Authors acknowledge the Gauss Center for Supercomputing (GCS) for providing computing time through the John von Neumann Institute for Computing (NIC) on the GCS share of the supercomputer JUQUEEN at the Jülich Supercomputing Center (JCS). R.Z.K. is grateful to the Swiss National Science Foundation for financial support and to the Swiss National Supercomputing Centre (CSCS) for computer time. T.D.K. acknowledges financial support from the Graduate School of Excellence MAINZ and the Carl Zeiss Foundation.

REFERENCES

(1) (a) Head-Gordon, T.; Hura, G. *Chem. Rev.* **2002**, *102*, 2651. (b) Bakker, H. J.; Skinner, J. L. *Chem. Rev.* **2010**, *110*, 1498. (c) Eisenberg, D.; Kauzmann, W. *The Structure and Properties of Water*; Clarendon: Oxford, 1969. (d) Paesani, F.; Voth, G. A. *J. Phys. Chem. B* **2009**, *113*, 5702.

(2) Stillinger, F. H. *Science* **1980**, *209*, 451.

(3) Clark, G. N. I.; Cappa, C. D.; Smith, J. D.; Saykally, R. J.; Head-Gordon, T. *Mol. Phys.* **2010**, *108*, 1415.

(4) Wernet, P.; Nordlund, D.; Bergmann, U.; Cavalleri, M.; Odelius, M.; Ogasawara, H.; Naslund, L. A.; Hirsch, T. K.; Ojamae, L.; Glatzel, P.; Pettersson, L. G. M.; Nilsson, A. *Science* **2004**, *304*, 995.

(5) Nilsson, A.; Pettersson, L. G. M. *Chem. Phys.* **2011**, *389*, 1.

(6) (a) Khaliullin, R. Z.; Cobar, E. A.; Lochan, R. C.; Bell, A. T.; Head-Gordon, M. *J. Phys. Chem. A* **2007**, *111*, 8753. (b) Khaliullin, R. Z.; Kühne, T. D. *Phys. Chem. Chem. Phys.* **2013**, *15*, 15746.

(7) Kühne, T. D.; Khaliullin, R. Z. *Nat. Commun.* **2013**, *4*, 1450.

(8) Habershon, S.; Manolopoulos, D. E.; Markland, T. E.; Miller, T. F., III. *Annu. Rev. Phys. Chem.* **2013**, *64*, 387.

(9) Spura, T.; John, C.; Habershon, S.; Kuehne, T. D. *arXiv:1402.1233* **2014** (Accessed Feb 12, 2014).

(10) (a) Morrone, J. A.; Car, R. *Phys. Rev. Lett.* **2008**, *101*, 017801. (b) Schmidt, J.; Vandevondele, J.; Kuo, I. F. W.; Sebastiani, D.; Siepmann, J. I.; Hutter, J.; Mundy, C. J. *J. Phys. Chem. B* **2009**, *113*, 11959.

(11) (a) Rottger, K.; Endriss, A.; Ihringer, J.; Doyle, S.; Kuhs, W. F. *Acta Crystallogr., Sect. B* **1994**, *50*, 644. (b) *CRC Handbook of Chemistry and Physics*; CRC Press: Boca Raton, FL, 2005.

(12) (a) Becke, A. D. *Phys. Rev. A* **1988**, *38*, 3098. (b) Lee, C. T.; Yang, W. T.; Parr, R. G. *Phys. Rev. B* **1988**, *37*, 785.

(13) Khaliullin, R. Z.; Bell, A. T.; Head-Gordon, M. *Chem.—Eur. J.* **2009**, *15*, 851.
(14) Agmon, N. *Acc. Chem. Res.* **2011**, *45*, 63.
(15) (a) Becke, A. D.; Edgecombe, K. E. *J. Chem. Phys.* **1990**, *92*, 5397. (b) Keutsch, F. N.; Saykally, R. J. *Proc. Natl. Acad. Sci. U.S.A.* **2001**, *98*, 10533.
(16) Kusalik, P. G.; Svishchev, I. M. *Science* **1994**, *265*, 1219.
(17) (a) Soper, A. K. *ISRN Phys. Chem.* **2013**, *2013*, 279463. (b) Skinner, L. B.; Huang, C.; Schlesinger, D.; Pettersson, L. G. M.; Nilsson, A.; Benmore, C. J. *J. Chem. Phys.* **2013**, *138*, 074506.
(18) (a) Zhang, C.; Donadio, D.; Gygi, F.; Galli, G. *J. Chem. Theory Comput.* **2011**, *7*, 1443. (b) Lin, I.-C.; Seitsonen, A. P.; Tavernelli, I.; Rothlisberger, U. *J. Chem. Theory Comput.* **2012**, *8*, 3902. (c) Gillan, M. J.; Alfe, D.; Bartok, A. P.; Csanyi, G. *arXiv:1303.0751* **2013**.
(19) Kong, L.; Wu, X.; Car, R. *Phys. Rev. B* **2012**, *86*, 134203.
(20) (a) Odelius, M.; Cavalleri, M.; Nilsson, A.; Pettersson, L. G. M. *Phys. Rev. B* **2006**, *73*, 024205. (b) Cavalleri, M.; Ogasawara, H.; Pettersson, L. G. M.; Nilsson, A. *Chem. Phys. Lett.* **2002**, *364*, 363.